# Numerical study of low-frequency vibrations in amorphous silicon

Joseph L. Feldman
*Naval Research Laboratory, Washington DC 20375-5345*

Philip B. Allen
*Department of Physics and Astonomy, State University of New York, Stony Brook, New York 11794-3800*

Scott R. Bickham
*Naval Research Laboratory, Washington DC 20375-5345*
*and Los Alamos National Laboratory, Los Alamos, New Mexico 87545*

(Received 29 July 1998)

Exact numerical vibrational eigenvectors and eigenvalues are studied for atomistic models of amorphous silicon ($a$-Si) with 216, 1000, and 4096 atoms in the periodic repeat unit. At the lowest frequencies, eigenvalues are sparse and eigenvectors are fairly plane-wave-like. However, some eigenvectors are ''quasilocalized'' or ''resonant.'' They are temporarily trapped in local regions of undercoordination. The present paper finds the following. (1) The ''quasilocalized'' modes are to a large extent artifacts of the finite size of the model systems. (2) The lower energy modes of realistic models in the harmonic approximation are broadened versions of the corresponding crystalline acoustic vibrations, with fairly well-defined wave vectors $Q$. The intrinsic broadening due to glassy disorder increases rapidly with $Q$, until at intermediate frequencies a meaningful $Q$ can no longer be assigned. (3) The intrinsic broadening due to disorder is strong enough to suppress thermal conductivity to the level seen experimentally, with no need for special anharmonic effects or localization, except for the influence of two-level systems on the modes at very low frequencies. (4) There is no inconsistency between the broadened propagating-wave description of low-energy modes and the occurrence of ''excess modes'' in specific heat or in spectra. However, amorphous silicon seems to have very few such excess modes. (5) ''Excess modes'' and the plateau in $\kappa(T)$ are not closely related, since the former is absent and the latter present in both experiment and in our calculations for $a$-Si. Our analysis agrees closely with the recent study of amorphous $SiO_2$ by Dell'Anna *et al.* [S0163-1829(99)08805-0]

## I. INTRODUCTION

The glassy phase of silicon is available only in films. Therefore there are fewer measurements of vibrations than for glassy $SiO_2$. However the structural simplicity of this single-component network glass has enabled realistic theoretical modeling, and we have now microscopic theories of vibrational properties such as mode diffusivity and thermal conductivity,[1,2] vibrational equilibration,[3,4] and thermal expansion.[5] At a theoretical level, the vibrations of amorphous silicon ($a$-Si) are quite well understood. These calculations are based on exact diagonalization of the dynamical matrix for the harmonic vibrations. The atomic coordinates were built by the Wooten-Weiner-Weaire (WWW) algorithm[6] and resemble closely the measured structure factors.[7,8] We use the interatomic force model of Stillinger and Weber.[9] The models used so far had 216 or 1000 silicon atoms in a periodically repeated cell. When eigenvectors are given periodic boundary conditions, these models have only sparse information about low-frequency vibrations. The lowest group of nonzero eigenvalues in these models corresponds roughly to crystalline transverse-acoustic vibrations at $\vec{Q}=(2\pi/a)(0.333,0,0)$ and $(0.2,0,0)$ respectively, and have energies $\approx 6$ meV and $\approx 4$ meV ($a$ is approximately the lattice constant of crystalline silicon, 5.43 Å). We did not previously attempt to extract information about low-energy vibrations from these models. The present paper includes eigenvectors and eigenvalues for a 4096-atom model,[10] whose lowest eigenvalues correspond to a crystalline $\vec{Q}$ at $(0.125,0,0)$ with a lowest energy $\approx 2$ meV. By combining information from all three models we propose and test a method to extrapolate to the large system limit.

Experimentally, glasses have several characteristic low-frequency anomalies, namely (i) quasielastic scattering attributed to relaxational motions,[11] (ii) a plateau in thermal conductivity $\kappa(T)$, (iii) excess specific heat or a bump in $C(T)/T^3$, and (iv) excess vibrational modes, or a bump in the density of states $D(\omega)/\omega^2$ seen in various spectroscopies. The recent development of inelastic x-ray scattering tools for long wavelengths and low energies[12–15] gives information which has reinvigorated the long-standing debate about these low-frequency anomalies, and motivates our work.

## II. VIBRATIONAL FREQUENCY DISTRIBUTION

Figure 1 shows eigenfrequency distributions $\mathcal{D}(\omega)$ calculated from three models of different sizes, using the formula

$$\mathcal{D}(\omega)=\frac{1}{\pi N}\sum_i \frac{\gamma}{(\omega-\omega_i)^2+\gamma^2}, \tag{1}$$

where the broadening $\gamma$ is chosen to be somewhat larger than the average level spacing. Except at very low and very high

 

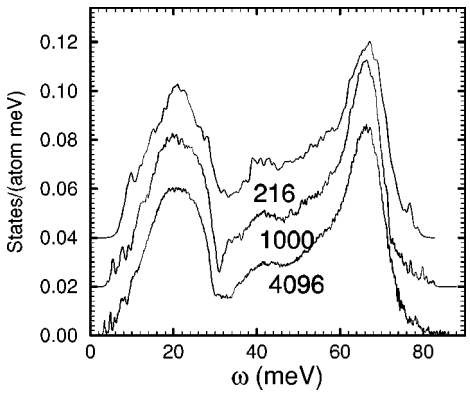


FIG. 1. Density of vibrational states of *a*-Si using the three models. Individual states are represented as Lorentzian lines with widths $\gamma = 0.5$, 0.2, and 0.1 meV [see Eq. (1)] for the 216-, 1000-, and 4096-atom model, respectively. All three models have a mobility edge near 72 meV, as can be seen for the 1000-atom model in Fig. 12.

frequencies, there is not much information in the larger models which is not already contained in the 216-atom model. The three models are very similar in character, but there are true differences in detail, as should be expected for finite-size pieces of a real glass. There is a close similarity to the spectra measured using neutrons by Kamitakara *et al.*[16] as shown in Fig. 2 of Ref. 2.

Figure 2 shows the same curves, blown up in the low-frequency region. The sparseness of low-energy modes is evident. The specific location of individual modes is accidental, but modes tend to cluster in ways which vary predictably as the size of the system changes. The aim of this paper is to investigate how predictable these features are, and then to use the predictability to extrapolate to the infinite system size.

### III. CONTROVERSIES OF INTERPRETATION

Lacking a good wave vector $\vec{Q}$ to label vibrational states, a theory of glassy vibrations must include new descriptive terms. The existing glossary contains terms such as ''boson peak'' and ''fracton'' which are poorly chosen since all harmonic vibrations qualify as bosons and since fractal properties are not present. There are also ambiguous terms such as ''phonon'' which is sometimes used as a generic term for all harmonic eigenstates, and sometimes as a specific term for states which propagate ballistically over a mean free path $\ell$ long enough that a wavelength $\lambda$ can be defined ($\ell > \lambda$). Finally there is confusion about the distinction between the Ioffe-Regel (I-R) crossover, where $\ell \approx \lambda$ and wave vectors become poorly defined, and Anderson localization. The latter term refers to a property of certain harmonic eigenstates that the eigenvectors $\hat{\epsilon}(\vec{R}_\ell)$ fall off exponentially in magnitude $\exp(-|\vec{R}_\ell - \vec{R}_0|/\xi)$ on a distance scale of a localization length $\xi$ from their center $\vec{R}_0$ of vibration. In harmonic approximation, such states contribute nothing to the heat conductivity $\kappa$. A sharp mobility edge $\omega_c$ separates these states from extended states. There is no theorem requiring extended states (which probably exist only in dimensionality $D > 2$) to have an approximate wave vector. In $D = 1$ or 2, the existence of an approximate wave vector $Q = 2\pi/\lambda$ does not protect a state from localization with $\xi \gg \lambda$, but in $D = 3$ an approximate wave vector **is** sufficient (but **not** necessary) to prevent localization.

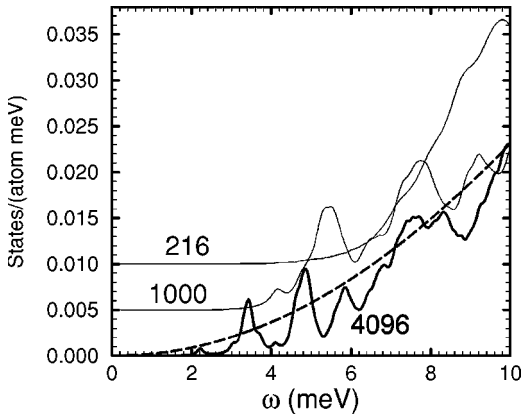


FIG. 2. Same as the previous figure except shown enlarged at low frequencies. The dashed line is the transverse phonon density of states extrapolated to infinite system size according to Eq. (6).

Corresponding to these descriptive ambiguities, both experiment and computer simulation have been given diametrically opposite interpretations by researchers looking at essentially equivalent information. On the theoretical side, the simulation of Guillot and Guisani[17] is consistent with the calculations of Dell'Anna *et al.*,[18] but ''excess modes'' are claimed in the former calculation and not in the latter. On the experimental side, the data of Foret *et al.*[15] are consistent with those of Masciovecchio *et al.*,[12–14] but Foret *et al.* claim evidence for acoustic localization, whereas Masciovecchio *et al.* see evidence for ballistic propagation. Since the average one-particle Green's function, and thus the dynamic structure factor, cannot distinguish Anderson-localized from delocalized states, Foret *et al.* cannot prove localization. We reinterpret their language to mean that the I-R crossover has been seen. This does not have a compulsory relationship to localization.

There is a clean theoretical distinction between localized and delocalized modes. For electrons, localization can be seen experimentally when the Fermi level lies within the band of localized states, because then the zero-temperature conductivity is zero. Conductivity at $T > 0$ shows activated hopping, but not activated number density or thermopower. For vibrations, experiments which probe the distinction between localized and delocalized states are not yet designed. One of the problems is that heat conduction involves the whole thermal spectrum of vibrations. At low energies (long wavelengths) vibrations are delocalized, so there is no possibility of an Anderson heat insulator.

We believe that a sharper language can diminish these ambiguities. The term ''excess modes'' is used here in place of ''boson peak,'' and the term ''phonon'' will not be used. We prefer[3] ''vibron'' as a generic term for harmonic normal modes, ''propagon'' for ballistically propagating modes, and ''locon'' (rather than fracton) for Anderson-localized modes. There are open arguments about how many other kinds of vibron occur in glasses. In our opinion (supported by detailed analysis[1–5,19–21] of *a*-Si; other workers, e.g., Ref. 22, find similar results for other glasses) the I-R crossover lies

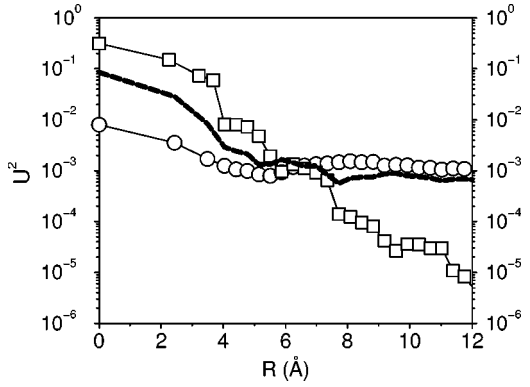


FIG. 3. Eigenvector profile from Ref. 29 of three selected eigenstates for the 1000-atom model of *a*-Si. $R=0$ corresponds to the atom where the eigenvector has maximum size. For $R>0$, averages over approximately spherical shells of atoms are made. The circles are for a typical diffuson, with $\omega=57$ meV and a participation ratio $P=500$. The squares show a highly localized state at $\omega=77$ meV and $P=6$. The filled line is a resonance at $\omega=6.5$ meV with $P=75$.

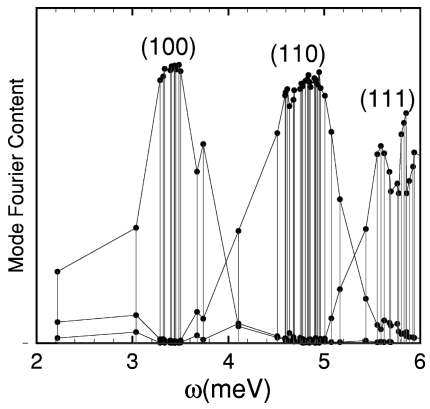


FIG. 4. For the lowest 65 modes of the 4096-atom model, this figure shows eigenfrequencies on the horizontal scale with vertical lines indicating transverse Fourier weights, Eq. (2), for the first three groups of wave vectors, $\vec{Q}=(2\pi/A)(1,0,0)$, etc. with $A=8a$ being the size of the cell.

fairly low in the spectrum, perhaps around 20 meV, while the mobility edge lies near the upper end, at 72 meV in our models. Therefore the majority of modes are neither ''propagons'' nor ''locons.'' These intermediate modes contribute to heat conductivity by a property of intrinsic diffusivity;[1,2] we call[3] them ''diffusons.'' Further discussion of terminology is in Appendix A. Cahill *et al.*[23] have reported a systematic study of thermal conduction of amorphous hydrogenated silicon films, which provides strong support for our ideas.

This leaves open a further question: are there still additional types of vibration at lower frequencies? The sparseness of low-frequency information in finite models makes this question challenging to answer numerically. A view advocated by Sokolov *et al.*,[24] which we test here, is that the excess modes at low frequency are contained in the propagon branch and arise from a strong frequency dependence of damping. Recently Schirmacher *et al.*[25] found softening of the transverse-acoustic peak of the vibrational density of states as a ''generic'' consequence of force-constant disorder. A third view holds that other kinds of modes such as ''resonant modes'' coexist with the propagons or lie in a band near the I-R crossover. A fourth view attributes excess modes to anharmonic vibrations in locally soft regions.[26,27] These views are not necessarily mutually exclusive, nor is it necessary that a single ''universal'' view should be equally correct for all glasses. For example, ''floppy modes''[28] are expected in underconstrained network glasses, but not in *a*-Si which is an overconstrained network glass. Our aim is to answer this question for the WWW model of *a*-Si.

''Resonant modes,'' like resonances in scattering theory or nuclear physics, are delocalized modes which have a large magnitude in a localized region and smaller magnitude (but not exponentially damped) elsewhere. The term ''quasilocalized'' is sometimes used. If prepared in an initially localized state, such a vibration will eventually tunnel out (in harmonic approximation) and propagate or diffuse away. Figure 3, taken from the Ph.D. thesis of Fabian,[29] shows the behavior of the squared magnitude of the vibrational eigenvector as a function of distance for some selected modes in *a*-Si. The distinction between localized and delocalized modes is clear. The distinction between resonant modes and other delocalized modes is less sharp and is a matter of judgement.

Agreeing with earlier work,[19,20] we find definite evidence for isolated resonant modes at low frequency in *finite* WWW models for *a*-Si. In recent work on thermal expansion[5] we discovered that these modes (which center on undercoordinated Si atoms) have anomalously large and usually negative Grüneisen parameters. In this paper we propose a method of extrapolation to infinite-size samples. According to this extrapolation, the resonant modes become less prominent as the sample size increases. In the infinite-size limit of homogeneous (no voids) *a*-Si, the resonant character of these long-wavelength modes is likely to disappear. The low-temperature thermal expansion is affected by these modes and will thus be hard to determine by a finite-size calculation.

## IV. DYNAMICAL STRUCTURE FACTOR

To what extent do the low-lying eigenvibrations of our models resemble the plane-wave Bloch states of a crystal? To answer this, we need to Fourier transform the eigenvectors $\vec{\epsilon}_i(\vec{R}_n)$ which give the pattern of the displacement vector on the atom $\vec{R}_n$ in normal mode $i$. The eigenvectors are normalized to one over the whole sample, $\Sigma_n|\vec{\epsilon}_i(\vec{R}_n)|^2=1$. Fourier wave vectors are chosen consistent with the periodic behavior of the eigenvectors in our supercell. We define transverse Fourier weights

$$C_T(\vec{Q},\mathrm{i})\equiv\frac{1}{2N_{\vec{Q}}}\sum_{T,\mathsf{R}}\left|\sum_n \vec{\epsilon}_T(\mathsf{R}\vec{Q})\cdot\vec{\epsilon}_i(\vec{R}_n)\exp(i\mathsf{R}\vec{Q}\cdot\vec{R}_n)\right|^2, \tag{2}$$

where $T$ labels two unit vectors $\epsilon_T(\vec{Q})$ which are perpendicular to $\vec{Q}$, and all $N_{\vec{Q}}$ vectors $\mathsf{R}\vec{Q}$ in the ''star'' of $\vec{Q}$ are averaged. The factor of 1/2 compensates for two transverse polarization directions. Appendix B discusses further the meaning of this formula. Figure 4 shows these Fourier components for the lowest normal modes of our biggest model.

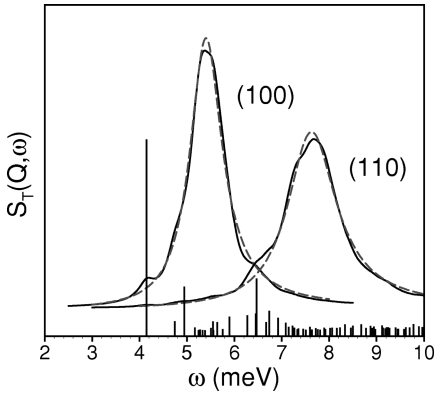


FIG. 5. Transverse structure factors, Eq. (3), plotted as a solid lines versus frequency for the 1000-atom model and for the lowest two groups of wave vectors. The delta functions in Eq. (3) were broadened into Lorentzians of width 0.2 meV. The dashed lines are Lorentzians, Eq. (4) fitted to the solid curves. The vertical lines starting on the frequency axis give the inverse participation ratios of the states, showing the quasilocalized or resonant nature of the lowest eigenstate at 4.2 meV.

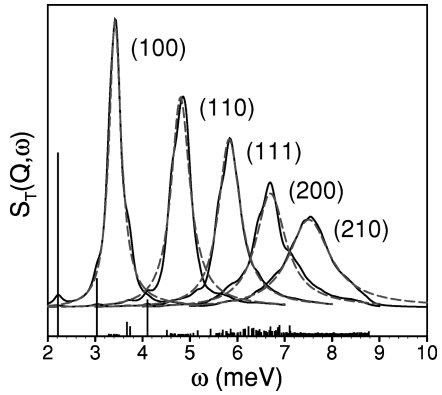


FIG. 6. Same as previous figure except for the 4096-atom model. Lorentzian broadening of 0.1 meV is used. At 4.1 meV a mode occurs which practically coincides with the lowest mode of the 1000-atom model, and is similarly quasilocalized. We now believe that this is an accidental coincidence and that all evidence for quasilocalization of harmonic modes will disappear in larger models as long as surfaces and voids are not present.

From this figure we see a striking regularity of behavior of the lowest eigenstates. The lowest group of wave vectors is six of the type $(2\pi/A)(1,0,0)$. In diamond structure silicon ($c$-Si) there are 12 corresponding degenerate modes (six wave vectors and two transverse polarizations). In $a$-Si we find ten closely spaced eigenfrequencies near 3.4 meV, which are built almost completely from this group of wave vectors, plus two modes at lower frequencies (2.2 and 3.0 meV) and two at higher frequency (both near 3.7 meV) which have mixed character but contain a lot of this lowest wave vector. The next lowest group, $(2\pi/A)(1,1,0)$, has 12 $TA_1$ and 12 $TA_2$ modes in $c$-Si. In Fig. 4 for $a$-Si, we see as expected that the two polarization types are not split. Twenty modes bunched near 4.8 meV are almost completely $(2\pi/A)(1,1,0)$ in character, and four more nearby have more than half of this character, with the tails out in both directions, especially to higher frequency. Further groups of wave vectors show similar behavior, with bunches of corresponding glassy modes, but less and less narrow in their frequency distribution.

Motivated by the x-ray structure factor, we define a quantity

$$S_T(\vec{Q},\omega)=\sum_i C_T(\vec{Q},i)\,\delta(\omega-\omega_i). \tag{3}$$

The corresponding longitudinal quantity is almost exactly what is measured by inelastic $x$-ray or neutron scattering. Graphs of these functions for the lowest few groups of wave vectors are shown in Fig. 5 for the 1000-atom model and in Fig. 6 for the 4096 atom model. The result is surprisingly smooth and symmetrical. A Lorentzian line

$$L_{\vec{Q}}(\omega)=A_{\vec{Q}}\,\mathrm{Im}\left[\frac{2\omega/\pi}{\omega^2-\omega_{\vec{Q}}^2-i\omega\Gamma_{\vec{Q}}}\right] \tag{4}$$

has been fitted to each structure function and is shown in the figures as dashed lines. The fits are reasonably good near the peak, but the calculated $S_T$ does not have as much weight as $L_{\vec{Q}}$ in the tail ($|\omega-\omega_{\vec{Q}}|>\Gamma_{\vec{Q}}$).

Also shown in Figs. 5 and 6 as vertical lines are the inverse participation ratios[30] $1/p_i$ of each mode. This quantity, discussed in our earlier paper [see Ref. 2, Eq. (3)], measures the degree of spatial localization of an eigenvector. The modes of mixed character which lie outside or in between the central groups of pure plane-wave modes are typically resonances as indicated by the large values of $1/p_i$. However, these modes are also reasonably well interpreted as filling in the appropriate tails of Lorentzian response functions, *modulo* small statistical fluctuations to be expected in finite systems.

## V. INTERPRETATION: RESONANT STATES OR PROPAGONS?

The eigenstates below and in between the pure plane-wave groups are quasilocalized or resonant; this is shown in Fig. 3 for a resonant mode which appears in Fig. 5 as a large $1/p_i$ at 6.5 meV. However, the evidence of Figs. 4, 5, and 6 plus further considerations given below lead us to believe that the resonant nature of this and similar states is an artifact of the finite size and will diminish in importance as the size of the system increases.

The Lorentzian fit of Eq. (4) gives three parameters, $\omega_Q$, $\Gamma_Q$, and $A_Q$ which characterize groups of normal modes. Figures 7, 8, and 9 show these parameters plotted versus $Q$. The evolution with $Q$ is smooth. Especially the frequency $\omega_Q$ is well behaved, yielding a transverse sound velocity of 3570 m/s. This agrees closely with the value 3670 m/s calculated independently for the same model by Feldman *et al.*[31] and cited in Ref. 2. There is a rigorous sum rule

$$\int_0^\infty d\omega S_T(\vec{Q},\omega)=1=\sum_i C_T(\vec{Q},i), \tag{5}$$

which for smaller $Q$ is well-fulfilled by the lowest 200 (1.6%) of the modes as shown by the filled circles and solid line in Fig. 9. The corresponding Lorentzian line should then

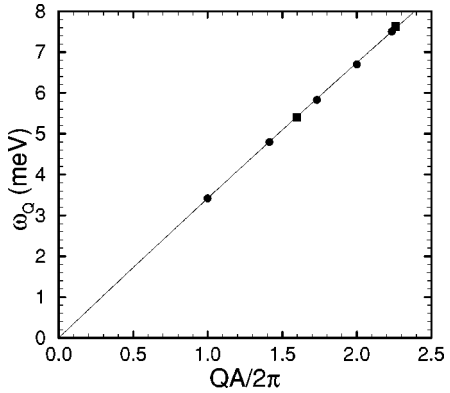


FIG. 7. Central frequency $\omega_Q$ versus wave vector $Q$ as extracted from the transverse structure factors shown in Figs. 5 (1000-atom model, filled squares) and 6 (4096-atom model, filled circles). The line corresponds to a transverse sound velocity of 3570 m/s.

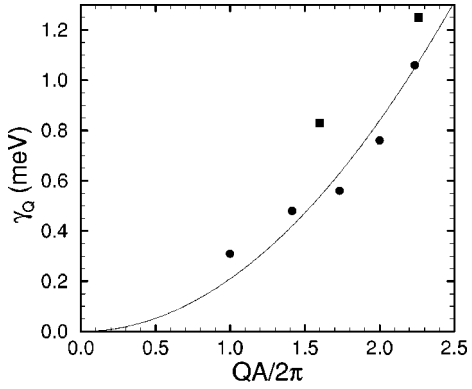


FIG. 8. Full width $\Gamma_Q$ at half maximum of the Lorentzian fits to the transverse structure factors. The solid line corresponds to the formula $\Gamma_Q = 0.21\ \text{meV}(QA/2\pi)^2$.

have $A_Q = 1$ if the sum rule is exhausted by the Lorentzian part of the spectral function. There are fluctuations of order 10% in the numerical values of $A_Q$ as shown in Fig. 9. One can attribute the irregularities of $\Gamma_Q$ and $A_Q$ to expected statistical fluctuations. There is also a systematically larger spectral weight in the Lorentzian areas $A_Q$ than in the computed spectral function, because in order to fit the peak, the Lorentzian is overestimating the size of the tails.

Notice that the resonant mode at 6.5 meV in the 1000-atom model (Fig. 5) is not resonant in the 4096-atom model (Fig. 6). This mode is in a gap between the Lorentzian structures centered at 5.5 and 7.7 meV in Fig. 5, whereas Fig. 6 has Lorentzian structures centered at 5.8 and 6.7 meV, leaving little gap for a state which does not ''belong'' to one of the plane-wave-like Lorentzian groups. Figure 8 shows that bigger models have widths of Lorentzian groups essentially as wide as smaller models. Therefore when models become bigger and small $|\vec{Q}|$'s become less sparse, Lorentzians of fixed width will overlap increasingly, and can force out the resonant states which otherwise would inhabit the gaps. For $|\vec{Q}|$ of order $1/L$ there will always be gaps, no matter how big the system $L$ (see for instance the region near 4.1 meV in Fig. 6 where a resonance occurs), but these gaps drift toward $|\vec{Q}| = 0$ and $\omega = 0$ as $L$ increases. Therefore the distinction between special frequencies lying in gaps, and other frequencies lying in Lorentzian peaks, must disappear as $L$ increases. There are two possibilities: either resonant behavior entirely disappears, or else it remains in a diluted form and is shared uniformly by all the normal modes. That is, at any given frequency there may be isolated parts of a large sample which are particularly sensitive to oscillation at just this frequency and temporarily trap selected traveling waves of this frequency. If this behavior is found for all normal modes, then any one normal mode will be freely propagating almost everywhere, and it becomes a subtle matter of definition or taste whether they should be called resonances at all.

Real glasses are less homogeneous than a large WWW network model, with internal voids. These will interact with long-wavelength modes in a fashion which we cannot predict from our calculations. Therefore, we cannot argue that resonances do not occur in real glasses, only that they do not seem to occur in homogeneous network models of the WWW type which model idealized homogeneous *a*-Si.

## VI. SPECIFIC HEAT AND EXCESS MODES

Many glasses show two kinds of anomalies in specific heat, (i) linear behavior $\gamma T$ at $T < 1$ K, and (ii) excess specific heat appearing as a greater bulge in a $C(T)/T^3$ vs $T$ curve than occurs in a corresponding crystal. The small sample size and large $\Theta_D$ of *a*-Si makes measurements difficult. The measurement of Mertig *et al.*[32] shows that $\gamma$, if present, is significantly smaller in *a*-Si than in $SiO_2$. It is customary to attribute the $\gamma T$ behavior to two-level systems. Measurements of internal friction by Liu *et al.*[33] did find a measureable density of two-level systems in pure amorphous silicon, but none in an hydrogenated sample. The measurement of Mertig *et al.* also shows that $C(T)/T^3$ *versus* $T$ is similar to crystalline Si except with a reduced $\Theta_D$ (from 645 to 528 K) and with the bulge setting in at lower $T$ (centered at 25 rather than 40 K). This indicates no thermally significant excess modes. Raman experiments[34,21] also fail to find excess modes in *a*-Si. Our normal mode calculations agree with this finding provided extrapolation to infinite size is made in a conservative fashion suggested by the results of the previous section.

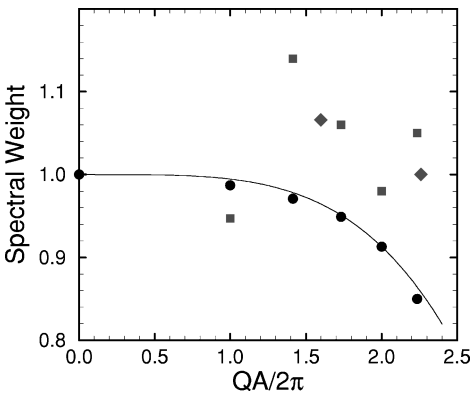


FIG. 9. Sum-rule fulfillment, Eq. (5) (right-hand version) from the lowest 200 normal modes, shown as filled circles, and areas $A_Q$ under the fitted Lorentzians (left-hand version), shown as filled squares (4096-atom model) and diamonds (1000-atom model). The curve corresponds to the formula $1 - 0.0054(QA/2\pi)^4$.

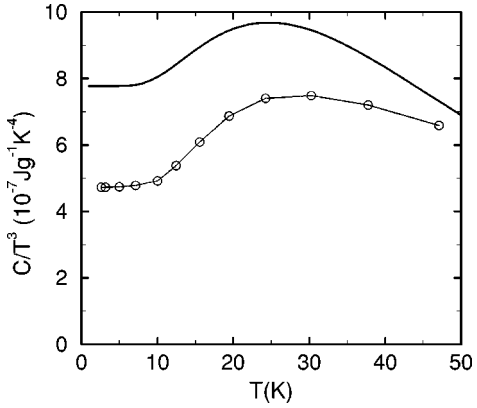


FIG. 10. Circles are measured values of $C(T)$ taken from Ref. 32. Calculations shown as the bold solid line use harmonic theory and the calculated density of states of Fig. 1 for $\omega > 6.35$ meV (4096-atom model) and $\Theta_D = 450$ K (Ref. 31) for $\omega < 6.35$ meV.

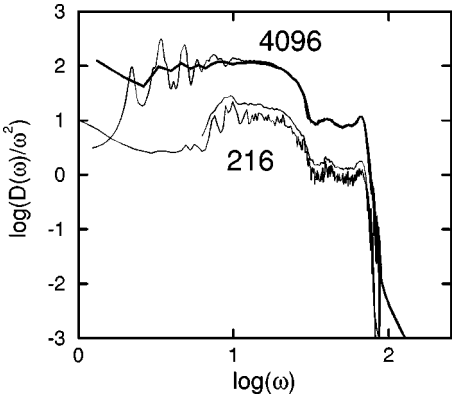


FIG. 11. Vibrational density of states by molecular dynamics (jagged lines) compared with exact diagonalization (smooth lines) for the smallest and largest models. A ratio of $D(\omega)$ to $\omega^2$ is shown in order to compare with a Debye model. The 216-atom model gives the false impression of excess modes near 10 meV energy. The vertical scale is arbitrary and has been shifted to separate the curves; logs are base 10 and $\omega$ is in meV.

The most conservative extrapolation is to argue that there are normal propagating modes at low frequencies whose spectrum, as in a crystal, is determined by the Debye temperature. Using the calculated elastic properties[31] $v_L = 7640$ m/s and $v_T = 3670$ m/s, we get a theoretical $\Theta_D$ for our model of 450 K. This is lower than the measured value 528 K of Mertig, presumably because of errors of the Stillinger-Weber interatomic forces. Using this extrapolation, the theoretical specific heat is compared with experiment in Fig. 10. The disagreement simply correlates with the discrepancy in Debye temperatures.

A less conservative extrapolation is to use not just the central frequency but also the width of the spectral functions calculated from the eigenvalues and eigenvectors in Sec. IV. The simplest formula is

$$\mathcal{D}(\omega) \cong \sum_{\vec{Q}} [2S_T(\vec{Q},\omega) + S_L(\vec{Q},\omega)] \sim \left(\frac{L}{2\pi}\right)^3 \int_0^{Q_D} 4\pi Q^2 dQ [2L_Q(\omega) + \text{longitudinal part}], \tag{6}$$

where $L_Q(\omega)$ is given in Eq. (4). The first version would be rigorous if the Fourier states formed an orthonormal basis. This is not true in a glass, as explained in Appendix B. The second version enables a smooth extrapolation at the cost of additional error. To implement Eq. (6) one must know the correct $Q$ dependence of $\Gamma_Q$. As shown in Fig. 8, the fitted values scatter too much to guide the extrapolation well. In principle, at very small $Q$ one should get a form $\Gamma_Q = CQ^4$ which corresponds to Rayleigh scattering of sound waves from the structural disorder. The data of Fig. 8 do not fit a $Q^4$ law; the $Q^2$ curve shown in the figure is a better fit. Two experiments[13,15] (but not a third[35]) and one calculation[18] on $a$-$SiO_2$ have also given $\Gamma \propto Q^2$. We do not know a theory which can give this law in a harmonic model. Using $\Gamma \propto Q^2$, we recalculated $C(T)/T^3$ by the extrapolation of Eq. (6). This enhances the density of states and the consequent specific heat by about 20% above the Debye value, increasing the discrepancy with experiment seen in Fig. 10 by 20%. Thus we think that the most conservative extrapolation is also the most reliable.

Sokolov *et al.*[24] have shown that the density of states obtained from the extrapolation of Eq. (6) can exhibit a bump, that is, excess modes, if the width $\Gamma_Q$ varies rapidly enough with $Q$. We have verified this and find it a plausible route to obtain the excess modes seen in many glasses. However, our values of $\Gamma_Q$ shown in Fig. 8 do not vary rapidly enough to produce such an effect, consistent with the experimental finding of no excess modes in $a$-Si.

Schirmacher *et al.*[25] proposed that excess modes result from a generic harmonic softening associated with force-constant disorder. Our model of amorphous silicon has such a softening, with the TA phonon peak in $\mathcal{D}(\omega)$ shifted from $\sim 25$ meV in crystalline (see Fig. 4 of Li *et al.*[36]) to $\sim 20$ meV in amorphous Si. However, this does not yield excess modes as seen in specific heat, so we think that generic softening, although real, is not the explanation.

Yet another way to obtain a density of states was used by Guillot and Guisani[17] to find excess modes in $a$-$SiO_2$. They did classical molecular-dynamics simulations and made a Fourier transform of the velocity-velocity correlation function. Since their conclusions differ from those of Dell'Anna[18] while their model should be similar, we have checked this method on $a$-Si. Our results are shown in Fig. 11. Our simulations were run at 30 K where atomic diffusion was negligible. The densities of states for both the 216-atom model and the 4096-atom model were essentially identical to those of Fig. 1 obtained by exact diagonalization of the same models. This indicates that anharmonic effects were small enough not to show up, yet large enough to permit vibrations to reach thermal equilibrium. The main point of Fig. 11 is that the 216-atom model shows a bump near 10 meV which is a size effect not appearing in the calculation of the 4096-atom model. This bump is pretty much the same as the feature seen in Ref. 17 near 50 $cm^{-1}$ on a sample containing 216 $SiO_2$ molecules. Therefore, we believe that their excess modes (''boson peak'') is a finite-size artifact. Since excess modes are known experimentally in $a$-$SiO_2$ (although it is

not known if they are harmonic) our point is not that existing models fail to show excess modes, but rather that extrapolating low-frequency information from finite-size models requires care. The correct prescription for extrapolation of harmonic information is not known, although we think that we have found the right one for models of *a*-Si.

## VII. THERMAL CONDUCTIVITY

In an insulator, heat is carried by thermal vibrations. The standard Peierls-Boltzmann theory (phonon-gas model) applies in a glass only at low $T$ where the thermally excited vibrations are propagons. In a crystal at low $T$ the mean-free path is as big as the sample and the thermal conductivity $\kappa(T)$ varies as $T^3$, following the specific heat. In a glass[37] the power law is closer to $T^2$ and requires a special scattering mechanism which can give a mean free path of the type $\ell \propto 1/T$. This caused Phillips[38] and Anderson *et al.*[39] to introduce the idea of ''two-level systems'' or ''tunneling systems'' which resonantly absorb sound waves at a rate proportional to the imbalance of population of the lower and upper levels, scaling as $1/T$. In a glass at higher $T$, vibrations are excited which no longer propagate ballistically, and the phonon-gas model no longer applies. Experimentally there is a ''plateau'' in the range 4 to 20 K, followed by an increase of $\kappa(T)$ which approximately follows the specific heat, saturating at higher temperature. Zaitlin and Anderson[40] showed that they could diminish $\kappa(T)$ at the plateau by introducing a dense array of small holes in the sample.

It is often stated that one needs an extremely strong mechanism to scatter propagons in a glass, in order to fit $\kappa(T)$ and to enable the plateau to develop. Therefore, we now check whether the Lorentzian broadening seen in our calculations is sufficiently strong to do this. The answer is yes.

The formula for heat conductivity is

$$\kappa(T)=\frac{1}{V}\sum_i D_i C(\hbar\omega_i/2k_BT), \tag{7}$$

where $D_i$ is the diffusivity of the $i$th normal mode of vibration and $C(x)$ is the specific heat of a harmonic oscillator, $C(x)=k_B(x/\sinh(x))^2$. This model works both in the phonon-gas model where $D_{\vec{Q}\lambda}=v^2_{\vec{Q}\lambda}\tau_{\vec{Q}\lambda}/3$ (states $i$ labeled by wave vectors), and in a purely harmonic model where $D_i$ is given by the vibrational analog of the Kubo-Greenwood formula derived by Allen and Feldman.[1] This latter formula can be computed using eigenvectors and eigenvalues of a finite-size model for those modes whose mean-free path is smaller than the size of the model. Figure 12 shows the results of this calculation (as reported in Ref. 1) for the diffusivity of the normal modes of the 1000-atom model. Also shown as a solid curve is the phonon gas model, where the fitted formula $1/\tau_Q=2\Gamma_i\propto Q_i^2$ is used for transverse propagons, and it is assumed that transverse and longitudinal propagons have the same diffusivity. Notice that the gas-model result fits perfectly onto the higher frequency diffuson result, indicating mutual consistency of the two different transport theories in the region of overlap 10 meV $<\omega<$20 meV.

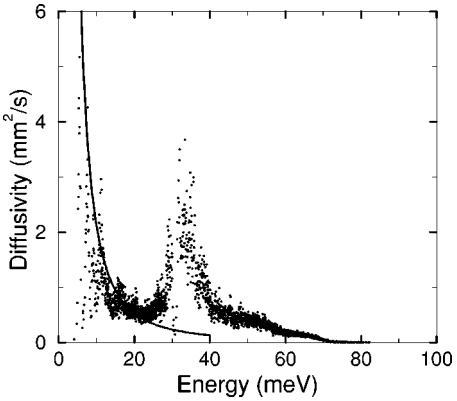


FIG. 12. Diffusivity $D_i$ of normal modes *versus* frequency for the 1000-atom model as calculated in Ref. 1, shown as solid dots. Note that $D_i$ goes to zero at 72 meV, the mobility edge, below the top of the spectrum at 82 meV. The low-frequency phonon-gas theory result is shown as a solid line and is the diffusivity of long-wavelength modes, $v^2\tau/3$, using $1/\tau=2\Gamma$ and taking $\Gamma$ from the smooth curve in Fig. 8.

Figure 13 shows $\kappa(T)$ calculated by inserting the diffusivity from Fig. 12 into Eq. (7). The theory lies below the data, as should be the case, since the harmonic decay at small $Q$ and $\omega$ has been overestimated by using $\Gamma\propto Q^2$. If we had used the correct Rayleigh $Q^4$ law, omitting the effect of sample boundaries, the low-frequency contribution would have diverged. Then introducing anharmonic scattering from two-level systems, a finite answer, larger than our result in Fig. 13 would result. As shown in Ref. 1 a satisfactory fit to the data can be produced by making appropriate amendments of this type.

The conclusion is that intrinsic harmonic glassy disorder contained in our finite calculation kills off the heat-carrying ability of propagons rapidly enough without invoking any exotic mechanism. Our $\kappa(T)$ curve is reminiscent of the experiments of Zaitlin and Anderson after holes are introduced to enhance the elastic damping of long-wavelength modes. The plateau disappears from their data in much the same way that it disappears from our theory due to extra damping of small-$Q$ propagons. We should also mention that our picture

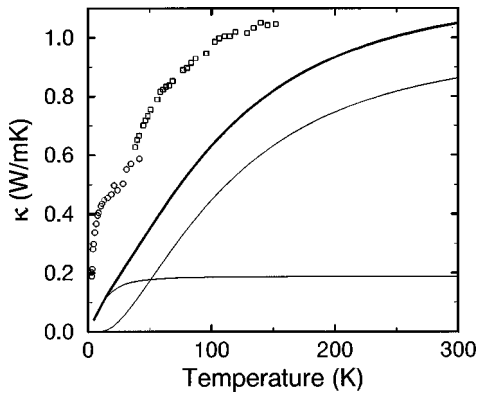


FIG. 13. The thin solid curve which saturates at lower $T$ is the contribution to $\kappa$ from propagons, using the solid curve from Fig. 12 for $\omega<6.35$ meV. The thin solid curve which saturates at higher $T$ is the contribution to $\kappa$ from diffusons, using the points from Fig. 12 for $\omega>6.35$ meV. The bold solid curve is the sum. Data at lower $T$ are from Pompe and Hegenbarth (Ref. 41) and at higher $T$ are from Cahill *et al.* (Ref. 42).

for the plateau, arising from the crossover between propagon heat currents and diffuson heat currents, is consistent with phenomenological models of Zaitlin and Anderson[40] and Graebner *et al.*[43].

## VIII. CONCLUDING REMARKS

The results shown here supplement our earlier work on higher energy properties and provide a comprehensive treatment of harmonic vibrations in *a*-Si. No excess modes are seen, and no low-energy localized or resonant modes survive in the large system limit. Of course, glasses contain low-energy anharmonic events like two-level system tunneling, which would not be accessible in any of our calculations except the molecular-dynamics simulations of Fig. 11. Both experiment and Fig. 11 suggest that such events are less important in *a*-Si than in other glasses. Our results are remarkably similar to a recent harmonic study of low-energy vibrations in *a*-$SiO_2$ by Dell'Anna *et al.*,[18] showing that our conclusions may be fairly general.

## ACKNOWLEDGMENTS

We thank B. Davidson for providing eigenvalues and eigenvectors of the 4096 atom model, and J. Fabian for providing Fig. 3. We thank I. Aleiner, G. Engel, J. Fabian, and D. Hess for helpful conversations. J.L.F. acknowledges support from the Office of Naval Research. The work of PBA was supported in part by NSF Grant No. DMR-9725037. S.R.B. acknowledges support by the NRC.

## APPENDIX A: DIFFUSONS

In Sec. III we define our terminology which attempts to solve some problems of nomenclature in glasses. We define[3] a ''diffuson'' as a delocalized eigenstate which does not propagate ballistically over any significant distance, but instead has an intrinsic diffusivity. The term ''diffuson'' is also used in the physics of weakly disordered electron systems,[44] where it denotes the particle-hole propagator,

$$\mathcal{N}(\epsilon)\mathcal{D}(\vec{r},\vec{r}',t)=\int\frac{d\omega}{2\pi}e^{-i\omega t}\langle G^A(\vec{r},\vec{r}';\epsilon)G^R(\vec{r}',\vec{r};\epsilon+\omega)\rangle \tag{A1}$$

with $\mathcal{N}(\epsilon)$ the density of states and $G^{A,R}$ advanced and retarded Green's functions. Over distances shorter than the elastic mean free path $\ell$ and times shorter than the inverse elastic scattering rate $\tau$, $\mathcal{D}$ has ballistic behavior

$$4\pi\mathcal{D}(\vec{r},\vec{r}',t)\approx(1/v_F t)^2\delta(|\vec{r}-\vec{r}'|-v_F t)\,\theta(t), \tag{A2}$$

while on longer length and time scales it goes to the diffusive form

$$4\pi\mathcal{D}(\vec{r},\vec{r}',t)\approx(1/Dt)^{3/2}\exp(-|\vec{r}-\vec{r}'|^2/4Dt)\,\theta(t). \tag{A3}$$

Here the diffusion constant $D=v_F\ell/3$ is the Fermi-surface average of the single-particle diffusivity $D_k=v_k^2\tau_k/3$. It determines the conductivity through the Einstein relation

$$\sigma=(e^2/\Omega)\sum_k D_k\delta(\epsilon_F-\epsilon_k)=e^2\mathcal{N}(\epsilon_F)D, \tag{A4}$$

where $\Omega$ is the volume. The particle called a ''diffuson'' in the present paper can also be called a ''single-particle diffuson'' to distinguish it from the ''particle-hole diffuson.'' The two kinds of diffuson bear some relationship. However, our diffusons have *no* ballistic behavior and thus lack any analog to Eq. (A2). We believe that a monoenergetic wave packet of our ''single-particle diffusons,'' initially located near point $\vec{r}$ at time $t=0$, behaves like Eq. (A3) at later times $t$ and positions $\vec{r}'$. The diffusivity $D_i$ cannot be meaningfully represented as $v_i^2\tau_i/3$ since $v_i$ and $\tau_i$ cannot be independently defined. Numerically we find that $D_i$ for diffusons is of order $\omega_D a/3$ where $a$ is the interparticle spacing. Also, $D_i$ is independent of the particular state $i$, depending only on the energy as seen in Fig. 12. Our Eq. (7) for the heat conductivity is a close analog of Eq. (A4).

## APPENDIX B: FOURIER REPRESENTATION OF GLASSY EIGENVECTORS

The vibrations of a system of $N$ atoms are $3N$ vectors $|u(t)\rangle$ whose components are the Cartesian components $\vec{u}_n(t)\cdot\hat{\alpha}$ of the displacement of the $n$th atom. The obvious basis for this vector space is the set of unit vectors $|n\alpha\rangle$ which ''point'' in the direction of the $\alpha$th component of the displacement of the $n$th atom. That is, they are column vectors with a single nonzero entry. Therefore $u_{n\alpha}(t)=\langle n\alpha|u(t)\rangle$. On a simple cubic lattice of volume $V=L^3=Na^3$, there is a unitary transformation to a new orthonormal basis $|\vec{Q}\lambda\rangle$ where

$$\langle n\alpha|\vec{Q}\lambda\rangle=\frac{1}{\sqrt{N}}\hat{p}_\lambda(\vec{Q})\cdot\hat{\alpha}\exp(i\vec{Q}\cdot\vec{R}_n). \tag{B1}$$

Here $\hat{p}_\lambda$ ($\lambda=1,2,3$) is a triad of orthogonal unit polarization vectors which can be chosen at will, and $\vec{Q}$ lies in the first Brillouin zone and has components $\vec{Q}=(2\pi/L)(h,k,l)$ which makes the displacements periodic with period $L$ in each primitive direction. When the vectors $\vec{R}_n$ are chosen to be the positions of the atoms in the model glass, the transformation is no longer unitary because the vectors $|\vec{Q}\lambda\rangle$ are no longer orthonormal. However, the vectors are still in general complete, so one can define left (L) and right (R) vectors of a biorthogonal set,

$$\langle\vec{Q}\lambda\mathrm{L}|\vec{Q}\lambda'\mathrm{R}\rangle=\delta_{\vec{Q}\vec{Q}'}\delta_{\lambda\lambda'},$$

$$\sum_{\vec{Q}\lambda}|\vec{Q}\lambda\mathrm{R}\rangle\langle\vec{Q}\lambda\mathrm{L}|=|\vec{Q}\lambda\mathrm{L}\rangle\langle\vec{Q}\lambda\mathrm{R}|=1, \tag{B2}$$

where the right vector is defined in Eq. (B1) and the left vector is constructed by inversion of the matrix $\langle n\alpha|\vec{Q}\lambda \mathrm{R}\rangle$. Therefore the vibrational eigenstates $|i\rangle$ can be represented as

$$|i\rangle = \sum_{\vec{Q}\lambda} |\vec{Q}\lambda \mathrm{L}\rangle\langle\vec{Q}\lambda \mathrm{R}|i\rangle. \tag{B3}$$

The quantity $|\langle\vec{Q}\lambda \mathrm{R}|i\rangle|^2$ can be regarded as the fraction of the normal mode $i$ which belongs to wave vector $\vec{Q}$ and polarization $\lambda$. The Fourier weights defined in Sec. IV, Eq. (2) can be rewritten in formal notation as

$$C_T(\vec{Q},\mathrm{i}) \equiv \frac{1}{2N_{\vec{Q}}} \sum_{T,\mathrm{R}} |\langle \mathrm{R}\vec{Q},T,\mathrm{R}|i\rangle|^2. \tag{B4}$$

These are what are plotted in Fig. 4. An alternative solution to the problem of nonorthogonality of the Fourier amplitudes has been proposed by Schulz and Handrich.[45]


[1] P. B. Allen and J. L. Feldman, Phys. Rev. B **48**, 12 581 (1993).
[2] J. L. Feldman, M. D. Kluge, P.B. Allen, and F. Wooten, Phys. Rev. B **48**, 12 589 (1993).
[3] J. Fabian and P. B. Allen, Phys. Rev. Lett. **77**, 3839 (1996).
[4] S. R. Bickham and J. L. Feldman, Phys. Rev. B **57**, 12 234 (1998); S. R. Bickham (unpublished).
[5] J. Fabian and P. B. Allen, Phys. Rev. Lett. **79**, 1885 (1997).
[6] F. Wooten, K. Winer, and D. Weaire, Phys. Rev. Lett. **54**, 1392 (1985).
[7] J. Fortner and J. S. Lannin, Phys. Rev. B **39**, 5527 (1989).
[8] S. Kugler, L. Pusztai, L. Rosta, P. Chieux, and R. Bellisent, Phys. Rev. B **48**, 7685 (1993).
[9] F. H. Stillinger and T. A. Weber, Phys. Rev. B **31**, 5262 (1985).
[10] J. L. Feldman, S. R. Bickham, G. E. Engel, and B. N. Davidson, Philos. Mag. B **77**, 507 (1998).
[11] U. Buchenau, H. M. Zhou, N. Nucker, K. S. Gilroy, and W. A. Phillips, Phys. Rev. Lett. **60**, 1318 (1988).
[12] C. Masciovecchio *et al.*, Phys. Rev. Lett. **76**, 3356 (1996).
[13] P. Benassi *et al.*, Phys. Rev. Lett. **77**, 3835 (1996); **78**, 4670 (1997).
[14] C. Masciovecchio *et al.*, Phys. Rev. B. **55**, 8049 (1997).
[15] M. Foret, E. Courtens, R. Vacher, and J.-B. Suck, Phys. Rev. Lett. **77**, 3831 (1996); **78**, 4669 (1997).
[16] W. A. Kamitakahara, C. M. Soukoulis, H. R. Shanks, U. Buchenau, and G. S. Grest, Phys. Rev. B **36**, 6539 (1987).
[17] B. Guillot and Y. Guisani, Phys. Rev. Lett. **78**, 2401 (1997).
[18] R. Dell'Anna, G. Ruocco, M. Sampoli, and G. Viliani, Phys. Rev. Lett. **80**, 1236 (1998).
[19] R. Biswas, A. M. Bouchard, W. A. Kamitakahara, C. M. Soukoulis, and G. S. Grest, Phys. Rev. Lett. **60**, 2280 (1988).
[20] A. M. Bouchard, R. Biswas, W. A. Kamitakahara, G. S. Grest, and C. M. Soukoulis, Phys. Rev. B **38**, 10 499 (1988).
[21] M. Marinov and N. Zotov, Phys. Rev. B **55**, 2938 (1997).
[22] V. Mazzacurati, G. Ruocco, and M. Sampoli, Europhys. Lett. **34**, 681 (1996).
[23] D. G. Cahill, M. Katiyar, and J. R. Abelson, Phys. Rev. B **50**, 6077 (1994).
[24] A. P. Sokolov, R. Calemczuk, B. Salce, A. Kisliuk, D. Quitmann, and E. Duval, Phys. Rev. Lett. **78**, 2405 (1997).
[25] W. Schirmacher, G. Diezemann, and C. Ganter, Phys. Rev. Lett. **81**, 136 (1998).
[26] V. G. Karpov, M. I. Klinger, and F. N. Ignatiev, Sov. Phys. JETP **57**, 439 (1983).
[27] U. Buchenau, Yu. M. Galperin, V. L. Gurevich, D. A. Parshin, M. A. Ramos, and H. R. Schober, Phys. Rev. B **46**, 2798 (1992).
[28] M. F. Thorpe, J. Non-Cryst. Solids **57**, 355 (1983).
[29] J. Fabian, Ph.D. thesis, SUNY, Stony Brook, New York, 1997.
[30] R. J. Bell and P. Dean, Discuss. Faraday Soc. **50**, 55 (1970).
[31] J. L. Feldman, J. Q. Broughton, and F. Wooten, Phys. Rev. B **43**, 2152 (1991).
[32] M. Mertig, G. Pompe, and E. Hegenbarth, Solid State Commun. **49**, 369 (1984).
[33] X. Liu, B. E. White, Jr., R. O. Pohl, E. Iwanizcko, L. M. Jones, A. H. Mahan, B. N. Nelson, R. S. Crandall, and S. Veprek, Phys. Rev. Lett. **78**, 4418 (1997).
[34] N. Maley, D. Beeman, and J. S. Lannin, Phys. Rev. B **38**, 10 611 (1988), and references therein.
[35] A. Wischnewski, U. Buchenau, A. J. Dianoux, W. A. Kamitakahara, and J. L. Zarestky, Phys. Rev. B **57**, 2663 (1998).
[36] X. P. Li, G. Chen, P. B. Allen, and J. Q. Broughton, Phys. Rev. B **38**, 3331 (1988).
[37] R. C. Zeller and R. O. Pohl, Phys. Rev. B **4**, 2029 (1971).
[38] W. A. Phillips, J. Low Temp. Phys. **7**, 351 (1972).
[39] P. W. Anderson, B. I. Halperin, and C. M. Varma, Philos. Mag. **25**, 1 (1972).
[40] M. P. Zaitlin and A. C. Anderson, Phys. Rev. B **12**, 4475 (1975).
[41] G. Pompe and E. Hegenbarth, Phys. Status Solidi B **147**, 103 (1988).
[42] D. G. Cahill, H. E. Fischer, T. Klitsner, E. T. Swartz, and R. O. Pohl, J. Vac. Sci. Technol. A **7**, 1259 (1989).
[43] J. E. Graebner, B. Golding, and L. C. Allen, Phys. Rev. B **34**, 5696 (1986).
[44] P. A. Lee and T. V. Ramakrishnan, Rev. Mod. Phys. **57**, 287 (1985).
[45] M. Schulz and K. Handrich, Phys. Status Solidi B **164**, 141 (1991).